Vertical distribution of microplastics in an agricultural soil after long-term treatment with sewage sludge and mineral fertiliser

Heinze, Wiebke Mareile; Steinmetz, Zacharias; Klemmensen, Nanna Dyg Rathje; Vollertsen, Jes; Cornelis, Geert

Published in:
Environmental Pollution

DOI (link to publication from Publisher):
10.1016/j.envpol.2024.124343

Publication date:
2024

Document Version
Publisher's PDF, also known as Version of record

Citation for published version (APA):
Heinze, W. M., Steinmetz, Z., Klemmensen, N. D. R., Vollertsen, J., & Cornelis, G. (2024). Vertical distribution of microplastics in an agricultural soil after long-term treatment with sewage sludge and mineral fertiliser. *Environmental Pollution*, *356*, Article 124343. https://doi.org/10.1016/j.envpol.2024.124343

Environmental Pollution 356 (2024) 124343

Contents lists available at ScienceDirect

Environmental Pollution

journal homepage: www.elsevier.com/locate/envpol

Vertical distribution of microplastics in an agricultural soil after long-term treatment with sewage sludge and mineral fertiliser☆

Wiebke Mareile Heinze [a], Zacharias Steinmetz [b], Nanna Dyg Rathje Klemmensen [c], Jes Vollertsen [c], Geert Cornelis [a,*]

[a] Swedish University of Agricultural Sciences, Department of Soil and Environment, Box 7014, 75007, Uppsala, Sweden
[b] RPTU Kaiserslautern-Landau, iES Landau, Institute for Environmental Sciences, Environmental and Soil Chemistry Lab, Fortstraße 7, 76829, Landau, Germany
[c] Aalborg University, Department of the Built Environment, Division of Civil and Environmental Engineering, Thomas Manns Vej 23, 9220, Aalborg, Denmark

ARTICLE INFO

Keywords:
Spatial distribution
Field scale
Transport
μ-FT-IR
Py-GC/MS
Metals
Organic carbon

ABSTRACT

Sewage sludge applications release contaminants to agricultural soils, such as potentially toxic metals and microplastics (MPs). However, factors determining the subsequent mobility of MPs in long-term field conditions are poorly understood. This study aimed to understand the vertical distribution of MPs in soils amended with sewage sludge in comparison to conventional mineral fertiliser for 24 years. The depth-dependent MP mass and number concentrations, plastic types, sizes and shapes were compared with the distribution of organic carbon and metals to provide insights into potentially transport-limiting factors. Polyethylene, polypropylene and polystyrene mass concentrations were screened down to 90 cm depth via pyrolysis-gas chromatography/mass spectrometry. MP number concentrations, additional plastic types, sizes, and shapes were analysed down to 40 cm depth using micro-Fourier transform-infrared imaging. Across all depths, MP numbers were twice and mass concentrations 8 times higher when sewage sludge was applied, with a higher share of textile-related plastics, more fibres and on average larger particles than in soil receiving mineral fertiliser. Transport of MPs beyond the plough layer (0–20 cm) is often assumed negligible, but substantial MP numbers (42 %) and mass (52 %) were detected down to 70 cm in sewage sludge-amended soils. The initial mobilization of MPs was shape- and size-dependent, because the fractions of fragmental-shaped and relatively small MPs increased directly below the plough layer, but not at greater depths. The sharp decline of total MP concentrations between 20 and 40 cm depth resembled that of metals and organic matter suggesting similar transport limitations. We hypothesize that the effect of soil management, such as ploughing, on soil compactness and subsequent transport by bioturbation and via macropores drives vertical MP distribution over long time scales. Risk assessment in soils should therefore account for considerable MP displacement to avoid underestimating soil exposure.

1. Introduction

Organic residues such as sewage sludge are typically applied to agricultural land to recycle nutrients. Other than a more efficient use of resources, sewage sludge also increases the carbon content of soils in contrast to conventional mineral fertilisers. However, sewage sludge may also release a range of potentially toxic metals (Chu and He, 2021; van Straalen et al., 1989) and, as recently highlighted, microplastics (MPs, ≤5 mm) to soils (Hurley and Nizzetto, 2018). Frequently occurring plastic types are polyesters (including polyethylene terephthalate, PET) and polyamides (PA), both commonly used in textiles, but also polyethylene (PE), polypropylene (PP) and polystyrene (PS) (Klemmensen et al., 2024). Most of these polymer types are resistant to biodegradation (Chamas et al., 2020) and may cause adverse effects in

Abbreviations: μ-FT-IR, micro-Fourier transform-infrared; DW, dry weight; K_d, partitioning coefficient; MP, microplastic; MPs, microplastics; Py-GC/MS, Pyrolysis-Gas Chromatography/Mass Spectrometry; PA, polyamides; PE, polyethylene; PET, polyethylene terephthalate; PP, polypropylene; PS, polystyrene; PTFE, polytetrafluoroethylene; WWTP, wastewater treatment plant.

☆ This paper has been recommended for acceptance by Eddy Y. Zeng.

* Corresponding author.
E-mail addresses: wiebkemareile.heinze@slu.se (W.M. Heinze), steinmetz-z@uni-landau.de (Z. Steinmetz), ndrk@build.aau.dk (N.D.R. Klemmensen), jesvollertsen@build.aau.dk (J. Vollertsen), geert.cornelis@slu.se (G. Cornelis).

https://doi.org/10.1016/j.envpol.2024.124343
Received 22 March 2024; Received in revised form 5 June 2024; Accepted 6 June 2024
Available online 7 June 2024

the long term either emerging from the plastics themselves or by releasing potentially toxic additives (Bucci et al., 2020; de Souza Machado et al., 2018). Transport processes may alter the distribution of both, MPs and metals, in the soil profile and thereby determine the local exposure concentrations of crops or terrestrial biota.

While it has been established that agricultural soils become enriched in MPs following sewage sludge applications (Corradini et al., 2019; Crossman et al., 2020; Ljung et al., 2018; Schell et al., 2022; Tagg et al., 2022; van den Berg et al., 2020; Zhang et al., 2020), there are still uncertainties about the subsequent mobility and further vertical distribution of MPs in agricultural soils, especially under long-term field conditions. Most of the existing field investigations on sewage sludge-amended soils have focused on the uppermost few centimetres of the soil assuming a limited mobility of MPs beyond the plough layer (Crossman et al., 2020; Ljung et al., 2018; Schell et al., 2022; Zhang et al., 2020). MPs may, however, be incorporated deeper into the soil by burrowing soil biota (Heinze et al., 2021; Huerta Lwanga et al., 2017; Rillig et al., 2017) and by transport with penetrating rainfall or irrigation water (Ren et al., 2021; X. Zhang et al., 2022; Zhao et al., 2022) or because of soil management, such as ploughing (Weber et al., 2022). MP properties, such as the polymer type (Gao et al., 2021; Koutnik et al., 2022), size (Dong et al., 2018; Qi et al., 2022; Ranjan et al., 2023) and shape (Han et al., 2022; X. Zhang et al., 2022), are thought to determine the magnitude of these transport processes and whether MPs are retained in the uppermost layers of the soils. Most of these aforementioned MP studies were laboratory-based and focused on isolated transport processes and thus, the obtained transport depths are not readily transferable to soils in the field. Factors facilitating or limiting MP transport in agricultural soils under long-term field conditions are still evasive. Transport of other soil constituents, such as metals and organic matter, is comparably better understood. While some metals can be transported in dissolved form, other metals are predominantly transported with preferential flow while bound to organic matter or mineral colloids (Moreira et al., 2022; Zheljazkov and Warman, 2004). Hence, comparing the distribution pattern of different metals or organic matter with that of MPs could facilitate the identification of factors that similarly control MP transport.

The overarching aim of this study was to understand the long-term vertical distribution of MPs in soil amended with sewage sludge in comparison to soil receiving conventional mineral fertiliser. MP analyses are often limited to either particle-based or mass-based methods, though both metrics are necessary for a comprehensive exposure assessment (Thomas et al., 2020; Thornton Hampton et al., 2022). We therefore measured MP mass and numbers directly by applying both a thermo-analytical and a spectroscopic method. We sampled soils from long-term field trials with these two fertiliser regimes and examined the mass-based distribution of MPs along the soil profile to 90 cm depth. For improving our understanding of potentially transport-limiting factors under long-term field conditions, we subsequently examined MP numbers and particle characteristics in the most enriched depth layers. Lastly, we compared the depth-distribution of MPs with that of organic matter and potentially toxic metals commonly associated with sewage sludge applications to provide insights into potentially soil-specific factors of transport dynamics. Our hypothesis was that MPs are redistributed in the soil profile by anthropogenic and natural transport processes, with transport distances decreasing with increasing MP size and elongated shapes.

2. Materials & methods

2.1. Field trials and soil properties

Soils were sampled at the Lanna long-term field trials, Skara, Sweden (N58.344, E13.104), in January 2021. Soils with two common agricultural fertilisation practices were compared: field plots with bi-annual application of municipal sewage sludge at rates of 8 tons dry weight (DW) ha^{-1} since 1996 (4 tons DW ha^{-1} $year^{-1}$, total 96 tons ha^{-1}), and annual application of conventional mineral fertiliser during the same period (80 kg ha^{-1} N as calcium nitrate, 40 kg ha^{-1} P, 30 kg ha^{-1} K). Each treatment comprised four replicate field plots with areas of 112 m^2 (8 × 14 m) except one field plot of the mineral fertiliser treatment with a smaller area (6 × 14 m). The plots had a minimum distance of 8 m relative to each other (see Supplementary Material S1 for a field map). Based on the maximum distance (120 m) between plots, the potential background contamination from diffuse microplastic sources may be assumed similar across plots. The difference in MP concentrations between the treatments can therefore be explained by differences in fertilisation inputs. Aboveground plant material was harvested each year, after which plots were fertilised and mouldboard-ploughed to a depth of ca. 20 cm. The dewatered and digested sewage sludge was sourced from nearby municipal wastewater treatment plants (WWTPs), with suppliers changing between years. In the autumn of 2020, the applied sewage sludge had a dry matter content of 18 % and an organic matter content of 62 % (loss on ignition). The dominant cropping system was spring-sowed oats and barley.

The soil at the site was classified as a *Eutric Cambisol* according to the World Reference Base (IUSS Working Group, 2015) with clay, silt and sand contents of 45 %, 47 % and 8 % in the plough layer (0–20 cm), and 61 %, 36 % and 3 % in deeper soil layers (20–40 cm) respectively (Kätterer et al., 2014), making it susceptible to compaction under management (Jarvis et al., 1991). The bulk density in the plough layer was lower for the sewage sludge-amended soil compared to the mineral fertiliser treated soil (1.30 g cm^{-3} versus 1.36 g cm^{-3}). For the soil below the plough layer, a bulk density of 1.5 g cm^{-3} was assumed for both treatments according to personal communication with the field station. The sewage sludge-amended soil was relatively acidic (pH 4.9) in comparison to the conventionally fertilised soil (pH 6.7) (Börjesson et al., 2014), and had a higher total organic carbon (TOC) content (2.28 ± 0.07 % versus 1.9 ± 0.1 %). For soils at this site, Jarvis et al. (1991) previously remarked the well-structured subsoil (0.3–0.7 m) dominated by angular aggregates, and the presence of biopores down to 1.0 m depth in their soil profile description. In 2021, an earthworm abundance of 150 individuals m^{-2} (2.8 g DW m^{-2}) was measured in the sewage sludge-amended soil, and 70 individuals m^{-2} (2.5 g DW m^{-2}) for the mineral fertiliser treatment (Viketoft et al., 2021).

2.2. Sampling and sample homogenization

Soil cores of 90 cm depth (diameter 2.5 cm) were used for determining the vertical distribution of MPs, selected metals, TOC and total nitrogen (N). In each field plot, 6–8 soil cores were taken at randomly selected positions. The cores were segmented into sections of 10 cm and mixed on-site, yielding one composite sample per depth segment for each replicate field plot (306–647 g DW, Supplementary Material S1). Samples from the uppermost 0–20 cm, corresponding to the plough layer, were pooled together given the probable homogenization of this layer ($n = 8$ per field, $n = 32$ per treatment). Samples were stored and air-dried in glass jars covered with aluminium foil. Then, approximately 200–300 g of the dried sample was homogenized with a mortar and pestle, and sieved to 2 mm.

2.3. Metal, organic carbon and total nitrogen analysis

Potentially toxic metals that are commonly associated with sewage sludge, i.e. cadmium (Cd), chromium (Cr), copper (Cu), nickel (Ni), lead (Pb) and zinc (Zn), were analysed using inductively coupled plasma sector field mass spectrometry following an acid extraction with *aqua regia* in a closed-vessel microwave system. For details on the procedure and quality control, see Supplementary Materials S2. TOC and total N were determined on 1.0 g subsamples using an elemental analyser (Leco, Tru-Mac). The mobility of metals in soils is often expressed by partitioning coefficients (K_d-values). We estimated the K_d value for Cu and Cd from the prevalent soil conditions (pH, TOC) for the sewage sludge-amended soil based on empiric correlation equations from the literature (Sauvé et al., 2000) to compare the potential mobility of these metals.

2.4. Microplastic analysis

We used a thermo-analytical method to screen the vertical mass distribution of the most frequent MP types (PE, PP, PS) to a depth of 90 cm, followed by a more in-depth analysis using micro-Fourier Transform-Infrared (μ-FT-IR) imaging on selected samples to capture a wider range of plastic types and to assess the effect of MP size and shape on transport dynamics. The combination of the two methods further allowed us to compare the relative contribution of different plastics in terms of particle mass and numbers.

2.4.1. Py-GC/MS

The mass-based distribution of PE, PP, and PS was measured to a depth of 90 cm using Py-GC/MS ($n = 32$ per treatment). The MP extraction and analysis procedure was largely based on Steinmetz et al. (2022, 2020). Briefly, 50 g soil underwent density separation using a saturated sodium chloride solution (1.19 g cm^{-3}, 250 mL) to selectively extract the target plastics (0.86–1.05 g cm^{-3}) reducing possible interferences. After shaking (4 h) and at least 16 h of sedimentation, the settled material was released and the supernatant was collected with cellulose filters (pore size 4–12 μm). The filters were transferred to culture tubes and plastics extracted with 1,2,4-trichlorobenzene and *p*-xylene (1:1, 7.76 mL) at 180 °C for 1 h with intermittent vortexing (0, 20, 40 min and after cooling). Then, 200 μL of the supernatant was spiked with deuterated polystyrene as internal standard (PS-d5, 4 μL of 5 mg L^{-1}). In contrast to Steinmetz et al. (2022), MP detection limits were decreased by analysing larger sample volumes (6 μL instead of 2 μL) by sequentially transferring 3 μL with intermittent air-drying (≥24 h) onto sample carriers. The resulting methodological limits of detection were 0.51 mg kg^{-1} for PE, 0.13 mg kg^{-1} for PP, and 0.02 mg kg^{-1} for PS (Supplementary Material S3).

Samples were pyrolyzed in a Pyroprobe 6150 filament pyrolyzer (CDS Analytical) and measured with a Trace GC Ultra (DSQII mass spectrometer, Thermo Fisher Scientific). Pyrolysis steps included an initial heating to 300 °C (3 min), followed by a flash pyrolysis at 700 °C (15 s, 10 K ms^{-1}) and a vent time of 3 min at 300 °C. The peaks used for quantification of PE, PP, and PS were 1,21-docosadiene, 2,4-dimethyl-1-heptene and styrene respectively. We used the open-source software OpenChrom for data processing (Wenig and Odermatt, 2010), with an automatic peak integration based on retention indices followed by a manual control (Steinmetz et al., 2022). All Py-GC/MS based results were corrected for negative controls and corrected for the daily drift using bracketing standards. For details on the general contamination control, setup and quality control for Py-GC/MS following reporting guidelines by Cowger et al. (2020) see Supplementary Material S3.

2.4.2. FPA-μ-FT-IR imaging

Focal plane array (FPA) μ-FT-IR imaging was used on separate subsamples for capturing particle sizes and shapes, as well as covering a wider range of plastic types. We chose to focus on the particle fraction <500 μm because these MPs are expected to be more mobile than larger MPs in soils. Soil samples (100 g) were selected based on MP concentrations from Py-GC/MS analyses, i.e. only depth segments between 0 and 40 cm ($n = 12$ per treatment). The sample preparations followed developed methods (Hurley et al., 2018; Liu et al., 2019; Löder et al., 2017), with deviations in the order of steps and reagents used. A higher density solution of zinc chloride (≥1.6 g cm^{-3}, 500 mL) than during the previous screening with Py-GC/MS was used to extract a wider range of MP types. Density separations were repeated three times for each sample, and the supernatant was filtered through a stainless-steel mesh (mesh width 10 μm). Organic material was removed by a sequence of hydrogen peroxide (H_2O_2, 10 %), sodium dodecyl-sulphate, protease (*Bacillus licheniformis*) and cellulase (*Aspergillus* sp) treatments. Particles ≥500 μm were removed with a test sieve, and the remaining sample was treated with a final H_2O_2 step and density separation. The supernatant was collected, rinsed, dried and re-suspended in 5.00 mL ethanol. For the field samples, 500–600 μL (10–12 % of total sample volume) were measured on zinc selenide windows with FPA-μ-FT-IR (Cary 670, Agilent Technologies, 128 × 128 FPA, wavelength range 850–3750 cm^{-1}, pixel resolution 5.5 μm). Procedural blanks revealed a potential contamination of 16 ± 15 particles per sample ($n = 3$), corresponding to 160 ± 150 particles kg^{-1}, and therefore a potential maximum error of 5.2% for the lowest detected concentration in field soils (3100 particles kg^{-1}).

After automatic processing in the freeware siMPle (Primpke et al., 2017, 2020a), the spectra of all detected MP particles were manually checked ($n = 10\,087$). Approximately 15 % of particles initially classified as MPs were rejected in this process due to potential interferences of other organic materials, the lack of unique peaks used for identification within the recorded IR range or a combination thereof. Plastic types with a relative frequency of less than 5 % in any sample were jointly classified as “other”. The setup was limited to MP sizes of 10–500 μm, based on filter and sieve mesh width. Large but thin fibres may still bypass the sieve, so detected particles larger than 500 μm were excluded from the analysis (1.7 % of all detected MPs). Particles were distinguished into fragments and fibres based on their aspect ratio, i.e. the ratio of the largest to the smallest Feret diameter. Particles with an aspect ratio ≥3.0 were classified as fibres (Cole, 2016; Zhang et al., 2022), all other particles were classified as fragments. For more details on protocols, quality control and a comprehensive list of detected plastic types see Supplementary Material S4.

2.4.3. Recovery tests for MP extraction

Recoveries of 48–53% for PS spheres (52 μm and 106 μm) were found previously for the μ-FT-IR method (Klemmensen et al., 2024). Recovery tests for Py-GC/MS analysis were done by spiking the target plastics (PE, PP, PS) at three different concentrations (5, 20, 40 mg kg^{-1}) into two soils (50 g): a fine-textured reference soil (RefeSol06 A) and a composite sample of the deeper soil layers of the mineral fertiliser treatment (60–90 cm). Average recoveries ranged from 30 to 70% at the lowest, and 50–100% at the highest spike concentration (Supplementary Table S6). Improved recoveries at higher spike concentrations may explain the lower recovery observed here in comparison to other studies with substantially higher spike concentrations (20 g kg^{-1} to 50 g kg^{-1}) (Okoffo et al., 2020). There was only little to weak evidence that recoveries were different between the soils (PE: $p = 0.17$, PP: $p = 0.07$, PS: $p = 0.9$). However, recoveries in the reference soil were more variable, which might indicate background contamination as reference soils are typically not processed with measures to prevent plastic contamination. While our recoveries were lower than expected, we still deemed the method suitable for screening purposes of PE, PP and PS.

2.5. Data processing and statistical analysis

Further data processing of the Py-GC/MS and μ-FT-IR data was done in R (version 4.3.0), see Supplementary Material S5 for a comprehensive overview of R packages used. For testing statistical significance, we used two-tailed t-tests ($\alpha = 0.05$) and reported the *p*-value according to recommendations (Wasserstein et al., 2019), unless *p*-values were below 0.001. For a more comprehensive assessment of MP presence and mobility in the soil, we compared the mass of PE, PP and PS as directly measured by Py-GC/MS with a mass estimate based on particle metrics obtained via μ-FT-IR imaging. We illustratively applied the conversion method incorporated into the siMPle software (Liu et al., 2019; Simon et al., 2018). In brief, the particle type-specific density is combined with size metrics, with the ratio of minor to major Feret diameter used to estimate particle thickness, assuming ellipsoid shapes for all but fibrous particles.

3. Results

3.1. Microplastic mass concentrations

Overall, the application of sewage sludge was associated with an enrichment of PE, PP, and PS in terms of mass concentration obtained by Py-GC/MS ($p = 0.003$) (Fig. 1), especially in the plough layer where concentrations ranged from 0.97 to 2.4 mg kg^{-1} (mean 1.47 ± 0.66 mg kg^{-1}). Concentrations in soils receiving mineral fertiliser overall were 8 times lower and even 25 times lower in the plough layer located at 0–20 cm depth, i.e. 0.00–0.09 mg kg^{-1} (mean 0.06 ± 0.04 mg kg^{-1}). To a large degree, this trend was caused by substantially higher PE concentrations in the sewage sludge treatment ($p = 0.001$).

MP mass concentrations generally decreased with depth, although the highest average mass concentration was found at 20–30 cm depth in sewage sludge-amended soils, largely due to high PS concentrations in one replicate field plot (Fig. 1). While MPs were detectable to depths of 60–70 cm in discrete instances, 48 % of the MP mass was detected in the plough layer, 37 % at 20–30 cm and 11 % at 30–40 cm for the sewage sludge-amended soil. Hence, only these depth segments were selected for in-depth analysis using μ-FT-IR imaging.

3.2. Microplastic number concentrations

MP number concentrations were measured via μ-FT-IR imaging for the depth segments 0–20, 20–30 and 30–40 cm as displayed in Fig. 2. Sewage sludge applications resulted in higher average particle numbers than mineral fertiliser applications (plough layer: averages 53 700 ± 5900 particles kg^{-1} versus 30 000 ± 37 000 particles kg^{-1}; $p = 0.002$). The unexpectedly high average concentrations in soils receiving mineral fertiliser were mostly due to one sample in which MP numbers were 5–12 times higher than in the other three replicate field plots (Fig. 2).

MP number concentrations were similar in the plough layer and in 20–30 cm depth sections for the sewage sludge-amended soils ($p = 0.4$), but then decreased to half at 30–40 cm depth ($p < 0.001$). Accordingly, 58 % of the total MP numbers in the sewage sludge treatment were found in the plough layer, 27 % were located in 20–30 cm and 14 % in 30–40 cm depth. Soils receiving mineral fertiliser showed a comparable distribution in terms of particle numbers with 57 %, 32 %, 11 % for 0–20 cm, 20–30 cm and 30–40 cm, when excluding the aforementioned highest value.

3.3. Depth-dependent distribution of microplastic types, shapes and sizes

The most abundant plastics found in the sewage sludge-amended soils are commonly associated with textiles (polyester, acrylic, polyamides; 63 %). While polyester was an important plastic type in both field treatments, PP, PS, and epoxy/phenoxy resins accounted for a larger proportion of all MPs when soils received mineral fertiliser (Fig. 2). There was no consistent depth-dependent pattern that would indicate preferential transport of a particular plastic type.

The majority of detected MPs were classified as fragments, but the proportion of fibres in sewage sludge-amended soil was higher (Table 1) and decreased from the plough layer to the underlying layers shown by decreasing aspect ratios ($p < 0.001$ for 20–30 cm). However, there was no evidence that shape differed at even greater depths for either treatments (sewage sludge: $p = 0.5$, mineral fertiliser $p = 0.9$).

Most of the MPs within the top 40 cm of the soil were <100 μm in size, i.e. 84 % of all particles in the mineral fertiliser, and 73 % for the sewage sludge treatment. Mean and median particle sizes were overall smaller in soils treated with mineral fertiliser than in soils treated with sewage sludge ($p < 0.001$, Table 1). MP sizes further decreased from the plough layer down to 20–30 cm for soils treated with mineral fertiliser ($p = 0.034$) and sewage sludge ($p < 0.001$). However, the size distributions within either treatment were very similar at greater depth (sewage sludge: $p = 0.8$; mineral fertiliser: $p = 0.9$). Interestingly, the size distribution showed plastic-type and treatment-dependent trends (Fig. 3). Polyester, PE and PP particles tended to be much larger than the other plastic types, but only in the sewage treated soils. PS and PA, in contrast, were much smaller with narrower size distributions.

3.4. Comparison of mass-based and number-based concentrations

Based on mass measurements of the sewage sludge-amended soil (Py-GC/MS), PE dominated and PS was primarily present in 20–30 cm depth sections, whereas PP concentrations were negligible. μ-FT-IR imaging conversely suggested that PP was as or even more important than PE in terms of particle numbers. Comparisons between mass-based and number-based methods are challenging but can be facilitated by particle-to-mass conversions based on size metrics obtained via μ-FT-IR.

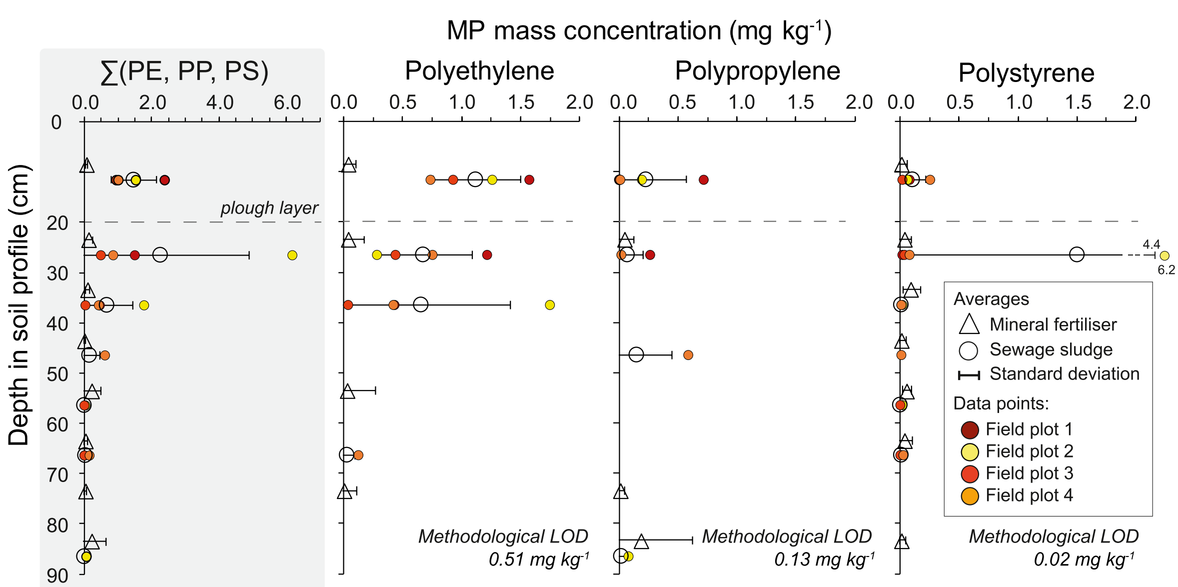

Fig. 1. Detected concentrations of polyethylene (PE), polypropylene (PP) and polystyrene (PS) according to sampling depth segments in sewage sludge and mineral fertiliser treatments in mass concentrations for Py-GC/MS (n = 4 for each treatment and depth).

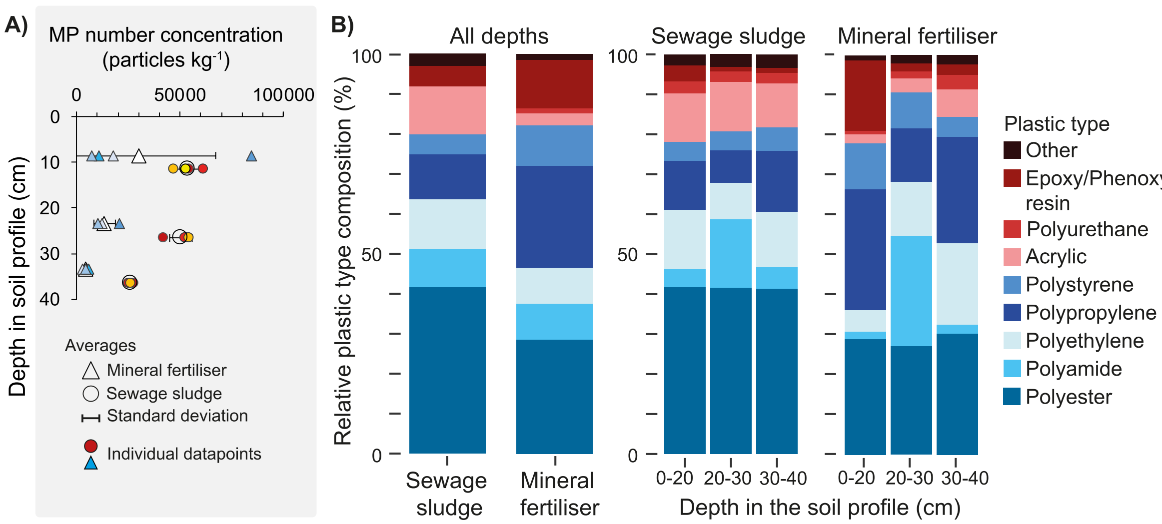

Fig. 2. MP number concentration (A) and plastic type composition (B) for sewage sludge-amended soil in comparison to soil receiving mineral fertiliser in 0–20, 20–30 and 30–40 cm depth in the soil profile.

Table 1
Treatment- and depth-dependent number based size and shape distribution of MPs in sewage sludge-amended soil and soil receiving mineral fertiliser.

	Depth (cm)	Size (μm)		Shape[a] (%)		Size classes (%) μm					
		Median	Mean	Fibre	Fragments	<50	50–100	100–200	200–300	300–400	400–500
Sewage sludge	0–20	66	101 ± 91	28.0	72.0	36	31	19.7	7.8	3.6	1.8
	20–30	54	84 ± 81	23.1	79.6	46	30	15.0	4.7	3.1	1.1
	30–40	56	85 ± 81	23.4	76.6	44	32	13.9	5.6	2.8	1.1
	All	**59**	**91 ± 86**	**25.2**	**74.8**	**42**	**31**	**16.7**	**6.1**	**3.3**	**1.4**
Mineral fertiliser	0–20	46	71 ± 71	13.5	86.5	55	28	10.9	4.3	1.2	1.0
	20–30	43	64 ± 65	14.2	85.8	62	24	9.1	3.1	1.6	0.5
	30–40	46	64 ± 60	14.0	86.0	57	28	10.8	2.7	0.9	0.5
	All	**45**	**68 ± 68**	**13.2**	**86.8**	**57**	**27**	**10.4**	**3.8**	**1.3**	**0.8**

[a] Classification based on aspect ratio (major to minor Feret diameter), <3 as fragment, >3 fibre.

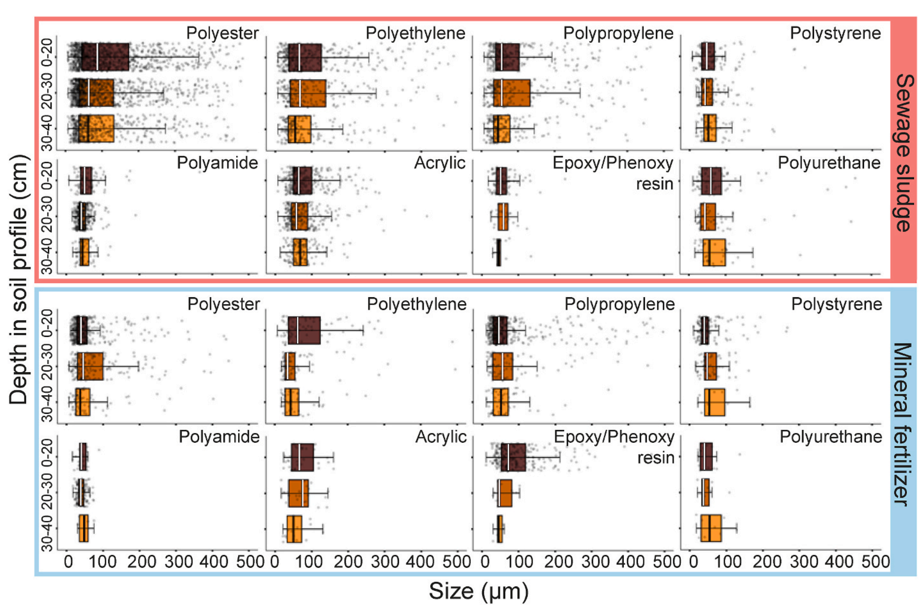

Fig. 3. Size distribution of the dominating plastic types (≥5% of all plastics in any one sample) according to depth segments (0–20, 20–30, 30–40 cm), for soils treated with sewage sludge and mineral fertiliser.

After particle-to-mass conversion, we found the relative importance of PE increased owing to on average larger particle sizes than PP (Fig. 3), whereas PS continued to play a minor role because small average particle sizes translated into small masses (Figs. 3 and 4). A lower size cut-off was used during sample preparing for the μ-FT-IR imaging method (500 μm) compared to that of the Py-GC/MS method (2 mm).

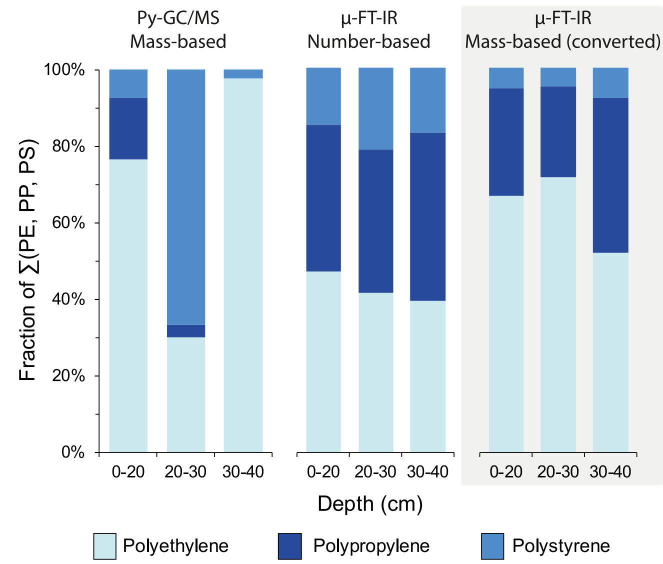

Fig. 4. Relative distribution of PE, PP and PS in sewage sludge-amended soil according to mass concentrations (mg kg^{-1}) measured using Py-GC-MS, number concentrations (particles kg^{-1}) measured using µ-FT-IR imaging and mass concentrations (mg kg^{-1}) estimated from µ-FT-IR-based size distributions by sampling depth.

Py-GC-MS was thus expected to yield higher mass concentrations than µ-FT-IR. However, mass concentrations for PE, PP, and PS estimated from particle-based size distributions generally exceeded the mass concentrations measured by Py-GC/MS, often by a factor of 2–4 (Supplementary Material S6).

3.5. Metal, organic carbon and nitrogen concentration and distribution

Unsurprisingly, sewage sludge applications increased the TOC, total N content and Cu ($p < 0.001$) and Zn ($p < 0.001$) concentrations in comparison to soils receiving mineral fertiliser, especially at 0–40 cm depth (Fig. 5). The concentrations of other metals commonly associated with sewage sludge, i.e. Cd, Cr and Ni were not noticeably affected by the different fertiliser regimes (Supplementary Material S2). The elevated Cd concentrations in the upper soil profile occurred similarly regardless of fertilisation practice ($p = 0.8$, Fig. 5).

For the sewage sludge amended soils, the concentrations of Cu, Cd, TOC, and total N concentrations were the highest between 0 and 30 cm depth, followed by a pronounced depth-dependent decline (Cu: $p < 0.001$, Cd: $p = 0.001$, TOC: $p = 0.001$, total N: $p < 0.001$). Notably, the vertical distribution of TOC, total N, Cu and Zn coincided with that of MPs (Fig. 1). K_d-values estimated based on pH and organic matter content were higher for Cu (920 L kg^{-1}) than for Cd (100 L kg^{-1}) in the sewage sludge-amended soil. Hence, a lower mobility is expected for Cu compared to Cd, mostly because of a stronger adsorption to organic matter at the prevailing soil conditions. Accordingly, the depth distribution of Cu coincided with that of TOC (Fig. 5), whereas Cd penetrated slightly deeper in the soil profile.

4. Discussion

4.1. Sewage sludge amendments caused enrichment of metals and microplastics in soil

Sewage sludge applications increased soil TOC and total N, but also led to an enrichment of potentially toxic metals and MPs when compared to conventional mineral fertiliser applications (Figs. 1, 2 and 5). Only Cu and Zn were elevated in response to sewage sludge applications (Fig. 5), but they remained below recommended maximum thresholds for Sweden (Naturvårdsverket, 2009). The total number concentrations of MPs were approximately twice and mass concentrations even 8 times higher when sewage sludge was used instead of mineral fertiliser. Although MPs found in soils treated with conventional fertiliser could originate from storage bags, we deem it more likely that they were transported from nearby field plots by ploughing, given the high MP concentrations in the sewage sludge-amended soils and the proximity between field plots (Figs. 1 and 2). Weber et al. (2022) recently attributed the spread of MPs from soils with a history of sewage sludge applications to ploughing activities with even larger transport distances of up to 40 m.

Both MP mass concentrations and number concentrations in our study were higher than previously reported for sewage sludge-amended soils. Field measurements of MP mass concentrations in soil are scarce (Steinmetz et al., 2022), and to our knowledge completely lacking for sewage sludge-amended soils. However, our measured concentrations (1.5 ± 0.6 mg kg^{-1}) exceed expected concentrations when combining previously reported MP mass concentrations for sewage sludge with the sludge application rate. For instance, based on PE concentrations in sewage sludge measured by Okoffo et al. (2020) (1.9 mg g^{-1} DW), we would expect only 0.07 mg kg^{-1} PE in our soil.

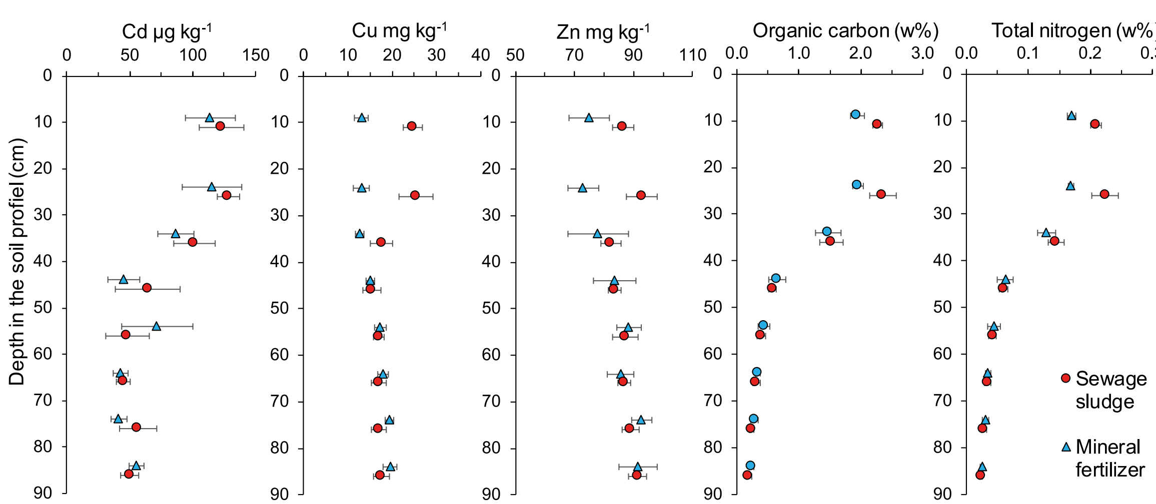

Fig. 5. Depth-dependent distribution of selected metals (cadmium, copper, and zinc), total organic carbon and total nitrogen in sewage sludge-amended soil in comparison to soil receiving mineral fertiliser.

Likewise, MP numbers were much higher than previously reported for sewage sludge-amended soils, ranging from 600 to 10 400 particles kg^{-1} (Corradini et al., 2019; Magnusson and Norén, 2014; Schell et al., 2022; van den Berg et al., 2020), and surpassed estimates based on MP numbers measured in sewage sludge and sludge application rates (Harley-Nyang et al., 2023). We infer that the lower size cut-off of our method (10 μm) partly explains the differences with other studies: 42–57 % of all MPs were below 50 μm in our study (Table 1). In comparison, Van den Berg et al. (2020) found ten times lower concentrations despite twice the amount of sewage sludge applied, but only reported numbers for particles >50 μm. Indeed, MP concentrations in our soils are within the expected range when estimating MP numbers based on recent sewage sludge measurements from Europe with a comparable lower size cut-off and quantification method (Chand et al., 2021; Horton et al., 2021). In addition, previous work on MP loads in sewage sludge has illustrated a high variability between sludge sourced from different WWTPs ranging between 644 and 5.8×10^6 particles kg^{-1} DW (Harley-Nyang et al., 2023). Such variability has been related to methodological differences between studies, but also different wastewater treatment steps and seasonal fluctuations of plastic inputs (Hooge et al., 2023; Li et al., 2018; Lofty et al., 2022). For instance, digested sludge, as was applied in our study, can contain higher MP numbers (Chand et al., 2021; Lares et al., 2018). Location-specific MPs loads might, for instance, explain that fragmental shaped MPs dominated in our study (Table 1), although sewage sludge is usually more associated with MP fibres (Corradini et al., 2019; Mahon et al., 2017).

4.2. Comparison of detected mass and number concentrations

In this study, we combined thermo-analytical and spectroscopic methods to directly measure MP mass and particle numbers for a more comprehensive assessment of MP concentrations in the soil. Unsurprisingly, the relative importance of the plastic types analysed with both methods (PE, PP, PS) depended on the presented metric because large quantities of small particles do not necessarily translate to large masses (Fig. 4). Conversion methods are commonly applied to translate particle sizes to particle masses for exposure assessments (Klemmensen et al., 2024). In terms of plastic mass concentrations, both analytical methods confirmed the importance of the on average larger sized PE MPs, and the minor role of the on average smaller PS MPs (Fig. 4). Discrepancies remained between the two methods concerning the role of PP, even after particle-to-mass conversion, likely related to analytical challenges of both methods: for Py-GC/MS with the quantification limit and μ-FT-IR imaging with the correct identification of PP. Weathering of PP can result in reduced signals in Py-GC/MS (Toapanta et al., 2021), though the effect on organic solvent-extracted PP detection is currently unclear. Furthermore, interferences and misclassification in μ-FT-IR imaging are potential sources for overestimating PP contents (Supplementary Material S4).

The comparison of directly measured MP mass with particle-based mass estimates also illustrated remaining challenges of conversion factors: Particle-derived MP masses greatly exceeded measured mass concentrations, a trend that was earlier reported for surface water and sediment samples (Primpke et al., 2020b; Viitala et al., 2022). While the omission of additives by Py-GC/MS can be a potential source for underestimating MP masses for some plastics, PE, PP and PS tend to contain only negligible concentrations of additives (Hahladakis et al., 2018). To address persisting uncertainties of conversion factors, further systematic comparisons of spectroscopic and thermo-analytical methods are necessary to understand the relationship between MP number, size and mass concentrations.

4.3. Microplastics are transported to soil depths below the plough layer

Sewage sludge application to agricultural soil is usually followed by ploughing that mixes sewage sludge and therefore organic matter, associated metals and MPs into the soil. Existing studies often assume a low mobility of MPs beyond this ploughed topsoil (Crossman et al., 2020). MP concentrations were indeed high in the plough layer (Figs. 1 and 2), but we were able to detect a substantial amount of MPs at greater depths in terms of mass (52 %) and number concentrations (42 %). Local variations in ploughing depth may have contributed to the presence of MPs, metals and organic matter at 20–30 cm depth. However, MPs found at greater depths up to 60–70 cm suggest continued transport in the soil profile by other transport processes.

In laboratory-based transport studies, MP mobility is often considered negligible (Alimi et al., 2018). Especially larger-sized (Dong et al., 2018; Ranjan et al., 2023) and fibrous MPs (Schell et al., 2022; X. Zhang et al., 2022) are typically considered largely immobile because of size exclusion, entanglement, straining or sedimentation. Indeed, we found a larger fraction of fragmental and smaller particles beyond 20 cm depth, but plastic type, as well as particle shape and size remained similar at greater depths (Table 1, Fig. 3). This lack of size- or shape-discrimination at greater depths can either be explained by the presence of macropores in which relatively large particles can still be transported by preferential flow or another less size-selective transport process. Burrowing soil biota play a vital role in the vertical redistribution of soil particles (Taylor et al., 2018). Earthworms, for instance, can transport particles as large as 5 mm through ingestion (McTavish and Murphy, 2021), potentially including MPs (Huerta Lwanga et al., 2017; Prendergast-Miller et al., 2019). Biopores at this site were previously found as far down as 1.0 m (Jarvis et al., 1991), making bioturbation-driven transport a likely process causing the observed transport distances of MPs. Similarly to other macropores, biopores can further facilitate the transport of relatively large particles to deeper parts of the soil profile (Jarvis et al., 2016; Leuther et al., 2023; Yu et al., 2019). MP transport in laboratory studies is accelerated and less size-restricted when processes such as bioturbation, drying-wetting or freeze-thawing cycles are included (Koutnik et al., 2022; O'Connor et al., 2019; Yu et al., 2019; X. Zhang et al., 2022; Zhao et al., 2022). These processes promote the development of connected macropores that can result in strong preferential flow, which was also observed for the clayey subsoils at the study site (Jarvis et al., 1991; Larsson and Jarvis, 1999). Consequently, bioturbation and preferential flow in macropores are likely causes for the observed translocation of even relatively large MPs in this agricultural soil.

The observed vertical MP transport in this and other field studies with soils under different management systems (Wahl et al., 2024; Weber et al., 2021) likely contributes to the reported discrepancies between estimated MP inputs, based on measurements in the initial sewage sludge in comparison to MP concentrations measured in soil plough layers (Crossman et al., 2020; Klemmensen et al., 2024). Neglecting vertical MP transport in sampling schemes can therefore result in a systematic underestimation of MP exposure of the soil ecosystem.

4.4. Microplastic and metal transport is affected by management

Although MPs were transported to the deeper soil, MP concentrations decreased considerably between 20 and 40 cm depth (Figs. 1 and 2). We suspect that this depth reflects the effect of heavy machinery and ploughing activities on the soil structure and pore connectivity below the plough layer, because similar depth distributions were found in other studies of agricultural cropland (Qiu et al., 2023; Tagg et al., 2022; Wahl et al., 2024; Weber and Opp, 2020). No-plough soils, such as grassland and riparian soils, often demonstrate more connected and deeper reaching soil pore systems (Larsbo et al., 2009; Torppa and Taylor, 2022), where indeed large MPs (2–5 mm) were found as deep as 60–90 cm in soil profiles reaching down 2 m (Weber and Opp, 2020).

Soil compactness can reduce plant rooting and the activity of earthworm burrowing (Arrázola-Vásquez et al., 2022; Capowiez et al., 2021), while annual tillage can disrupt deep-burrowing earthworm species, and the soil pore connectivity (Capowiez et al., 2009). Transport dynamics can thus be affected directly by soil management, through decreased water movement (Schlüter et al., 2020), and indirectly through a changed behaviour of soil biota (Blanchy et al., 2023; Jégou et al., 2002; Keller et al., 2017). The previously recorded strong decrease in hydraulic conductivity in soils at our study site between 15 and 30 cm depth (Jarvis et al., 1991) may indicate such compaction. While this measurement was done ca. 30 years before samples were taken for the current study, continued agricultural activity would be expected to further increase these trends. The depth distribution of other soil constituents likewise suggested reduced transport dynamics at greater depths (Fig. 5). For instance, the sharp decrease of TOC not only coincided with the distribution of MPs (30–40 cm, Fig. 5), but is also characteristic for mouldboard-ploughing systems with compact layers below the plough layer (Martínez et al., 2016; Zhou et al., 2023). The distribution of Cu largely followed that of TOC, Cd, in contrast, is expected to transport in dissolved form both in macro- and micropores, explaining its slightly higher mobility in the soil. Hence, although agricultural management practices did not completely restrict transport dynamics of MPs, TOC and metals entering the soil via external sources, it likely explains why transport distances of MP in agricultural soils were on average lower compared to MPs in other land uses such as grassland (Weber and Opp, 2020).

5. Implications and conclusion

24 years of sewage sludge applications to agricultural soil increased soil TOC but also led to a higher exposure to MPs and potentially toxic metals as compared to soils receiving mineral fertiliser. The measured MP particle and mass concentrations exceeded previously reported values, likely because of methodological differences and variations in MP contents in applied sewage sludges. The relative contribution of different plastic types depended on the measured metric, i.e. mass or number concentration, highlighting the need for measuring both for a comprehensive assessment. Long-term exposure to field conditions facilitated the vertical transport of a substantial fraction of particularly relatively small, fragmentally shaped MPs below the plough layer, likely facilitated by burrowing soil biota and connected macropores. Neglecting vertical MP transport during long-term projections of MP exposure therefore results in a systematic underestimation of MPs present in the whole soil ecosystem. Despite the observed transport, concentrations of MPs, TOC and metals all decreased sharply between 20 and 40 cm depth; a depth that is indicative of compaction in response to agricultural soil management practices like ploughing. Hence, there is a further need to improve our understanding of the interactions between soil structure, soil management and MP properties to assess their long-term fate in agricultural soils reliably.

Funding

This work was supported by ACEnano (EU Horizon 2020; grant agreement no. 720952), the Swedish research council FORMAS (project no. 2018–01080), Horizon 2020 European Join Program (EJP) Soil (project no. 862695) - WP3 project EOM4Soil, the Swedish University of Agricultural Sciences, RPTU Kaiserslautern-Landau and Aalborg University.

CRediT authorship contribution statement

Wiebke Mareile Heinze: Writing – review & editing, Writing – original draft, Visualization, Validation, Methodology, Investigation, Formal analysis, Conceptualization. **Zacharias Steinmetz:** Writing – review & editing, Validation, Software, Methodology, Investigation, Formal analysis. **Nanna Dyg Rathje Klemmensen:** Writing – review & editing, Methodology, Investigation, Formal analysis. **Jes Vollertsen:** Writing – review & editing, Supervision, Methodology. **Geert Cornelis:** Writing – review & editing, Supervision, Funding acquisition, Conceptualization.

Declaration of competing interest

The authors declare that they have no known competing financial interests or personal relationships that could have appeared to influence the work reported in this paper.

Data availability

Data will be made available on request.

Acknowledgements

Special thanks to Nora Ottander and Silvia Eichhöfer who provided much support during the laboratory analysis, to Sofia Delin and Lanna research station, and to Tobias Klöffel, Maarten Wynants and Katrin Rychel for feedback.

Appendix A. Supplementary data

Supplementary data to this article can be found online at https://doi.org/10.1016/j.envpol.2024.124343.

References

Alimi, O.S., Farner Budarz, J., Hernandez, L.M., Tufenkji, N., 2018. Microplastics and nanoplastics in aquatic environments: aggregation, deposition, and enhanced contaminant transport. Environ. Sci. Technol. 52, 1704–1724. https://doi.org/10.1021/acs.est.7b05559.

Arrázola-Vásquez, E., Larsbo, M., Capowiez, Y., Taylor, A., Sandin, M., Iseskog, D., Keller, T., 2022. Earthworm burrowing modes and rates depend on earthworm species and soil mechanical resistance. Appl. Soil Ecol. 178, 104568 https://doi.org/10.1016/j.apsoil.2022.104568.

Blanchy, G., Bragato, G., Di Bene, C., Jarvis, N., Larsbo, M., Meurer, K., Garré, S., 2023. Soil and crop management practices and the water regulation functions of soils: a qualitative synthesis of meta-analyses relevant to European agriculture. SOIL 9, 1–20. https://doi.org/10.5194/soil-9-1-2023.

Börjesson, G., Kirchmann, H., Kätterer, T., 2014. Four Swedish long-term field experiments with sewage sludge reveal a limited effect on soil microbes and on metal uptake by crops. J. Soils Sediments 14, 164–177. https://doi.org/10.1007/s11368-013-0800-5.

Bucci, K., Tulio, M., Rochman, C.M., 2020. What is known and unknown about the effects of plastic pollution: a meta-analysis and systematic review. Ecol. Appl. 30, e02044 https://doi.org/10.1002/eap.2044.

Capowiez, Y., Cadoux, S., Bouchant, P., Ruy, S., Roger-Estrade, J., Richard, G., Boizard, H., 2009. The effect of tillage type and cropping system on earthworm communities, macroporosity and water infiltration. Soil Tillage Res. 105, 209–216. https://doi.org/10.1016/j.still.2009.09.002.

Capowiez, Y., Sammartino, S., Keller, T., Bottinelli, N., 2021. Decreased burrowing activity of endogeic earthworms and effects on water infiltration in response to an increase in soil bulk density. Pedobiologia 85–86, 150728. https://doi.org/10.1016/j.pedobi.2021.150728.

Chamas, A., Moon, H., Zheng, J., Qiu, Y., Tabassum, T., Jang, J.H., Abu-Omar, M., Scott, S.L., Suh, S., 2020. Degradation rates of plastics in the environment. ACS Sustain. Chem. Eng. 8, 3494–3511. https://doi.org/10.1021/acssuschemeng.9b06635.

Chand, R., Rasmussen, L.A., Tumlin, S., Vollertsen, J., 2021. The occurrence and fate of microplastics in a mesophilic anaerobic digester receiving sewage sludge, grease, and fatty slurries. Sci. Total Environ. 798, 149287 https://doi.org/10.1016/j.scitotenv.2021.149287.

Chu, L., He, W., 2021. Toxic metals in soil due to the land application of sewage sludge in China: Spatiotemporal variations and influencing factors. Sci. Total Environ. 757, 143813 https://doi.org/10.1016/j.scitotenv.2020.143813.

Cole, M., 2016. A novel method for preparing microplastic fibers. Sci. Rep. 6, 34519 https://doi.org/10.1038/srep34519.

Corradini, F., Meza, P., Eguiluz, R., Casado, F., Huerta-Lwanga, E., Geissen, V., 2019. Evidence of microplastic accumulation in agricultural soils from sewage sludge disposal. Sci. Total Environ. 671, 411–420. https://doi.org/10.1016/j.scitotenv.2019.03.368.

Cowger, W., Booth, A.M., Hamilton, B.M., Thaysen, C., Primpke, S., Munno, K., Lusher, A.L., Dehaut, A., Vaz, V.P., Liboiron, M., Devriese, L.I., Hermabessiere, L., Rochman, C., Athey, S.N., Lynch, J.M., De Frond, H., Gray, A., Jones, O.A.H., Brander, S., Steele, C., Moore, S., Sanchez, A., Nel, H., 2020. Reporting guidelines to increase the reproducibility and comparability of research on microplastics. Appl. Spectrosc. 74, 1066–1077. https://doi.org/10.1177/0003702820930292.

Crossman, J., Hurley, R.R., Futter, M., Nizzetto, L., 2020. Transfer and transport of microplastics from biosolids to agricultural soils and the wider environment. Sci. Total Environ. 724, 138334 https://doi.org/10.1016/j.scitotenv.2020.138334.
de Souza Machado, A.A., Lau, C.W., Till, J., Kloas, W., Lehmann, A., Becker, R., Rillig, M. C., 2018. Impacts of microplastics on the soil biophysical environment. Environ. Sci. Technol. 52, 9656–9665. https://doi.org/10.1021/acs.est.8b02212.
Dong, Z., Qiu, Y., Zhang, W., Yang, Z., Wei, L., 2018. Size-dependent transport and retention of micron-sized plastic spheres in natural sand saturated with seawater. Water Res. 143, 518–526. https://doi.org/10.1016/j.watres.2018.07.007.
Gao, J., Pan, S., Li, P., Wang, L., Hou, R., Wu, W.-M., Luo, J., Hou, D., 2021. Vertical migration of microplastics in porous media: Multiple controlling factors under wet-dry cycling. J. Hazard Mater. 419, 126413 https://doi.org/10.1016/j.jhazmat.2021.126413.
Hahladakis, J.N., Velis, C.A., Weber, R., Iacovidou, E., Purnell, P., 2018. An overview of chemical additives present in plastics: migration, release, fate and environmental impact during their use, disposal and recycling. J. Hazard Mater. 344, 179–199. https://doi.org/10.1016/j.jhazmat.2017.10.014.
Han, N., Zhao, Q., Ao, H., Hu, H., Wu, C., 2022. Horizontal transport of macro- and microplastics on soil surface by rainfall induced surface runoff as affected by vegetations. Sci. Total Environ. 831, 154989 https://doi.org/10.1016/j.scitotenv.2022.154989.
Harley-Nyang, D., Memon, F.A., Osorio Baquero, A., Galloway, T., 2023. Variation in microplastic concentration, characteristics and distribution in sewage sludge & biosolids around the world. Sci. Total Environ. 891, 164068 https://doi.org/10.1016/j.scitotenv.2023.164068.
Heinze, W.M., Mitrano, D.M., Lahive, E., Koestel, J., Cornelis, G., 2021. Nanoplastic transport in soil via bioturbation by Lumbricus terrestris. Environ. Sci. Technol. 55, 16423–16433. https://doi.org/10.1021/acs.est.1c05614.
Hooge, A., Hauggaard-Nielsen, H., Heinze, W.M., Lyngsie, G., Ramos, T.M., Sandgaard, M.H., Vollertsen, J., Syberg, K., 2023. Fate of microplastics in sewage sludge and in agricultural soils. TrAC, Trends Anal. Chem. 166, 117184 https://doi.org/10.1016/j.trac.2023.117184.
Horton, A.A., Cross, R.K., Read, D.S., Jürgens, M.D., Ball, H.L., Svendsen, C., Vollertsen, J., Johnson, A.C., 2021. Semi-automated analysis of microplastics in complex wastewater samples. Environ. Pollut. 268, 115841 https://doi.org/10.1016/j.envpol.2020.115841.
Huerta Lwanga, E., Gertsen, H., Gooren, H., Peters, P., Salánki, T., Ploeg, M. van der, Besseling, E., Koelmans, A.A., Geissen, V., 2017. Incorporation of microplastics from litter into burrows of Lumbricus terrestris. Environ. Pollut. 220, 523–531. https://doi.org/10.1016/j.envpol.2016.09.096.
Hurley, R.R., Lusher, A.L., Olsen, M., Nizzetto, L., 2018. Validation of a method for extracting microplastics from complex, organic-rich, environmental matrices. Environ. Sci. Technol. 52, 7409–7417. https://doi.org/10.1021/acs.est.8b01517.
Hurley, R.R., Nizzetto, L., 2018. Fate and occurrence of micro(nano)plastics in soils: knowledge gaps and possible risks. Curr. Opin. Environ. Sci. Health 1, 6–11. https://doi.org/10.1016/j.coesh.2017.10.006.
IUSS Working Group, 2015. World Reference Base for Soil Resources 2014, Update 2015: International Soil Classification System for Naming Soils and Creating Legends for Soil Maps. World Soil Resource Reports FAO.
Jarvis, N., Bergström, L., Dik, P.E., 1991. Modelling water and solute transport in macroporous soil. II. Chloride breakthrough under non-steady flow. J. Soil Sci. 42, 71–81. https://doi.org/10.1111/j.1365-2389.1991.tb00092.x.
Jarvis, N., Koestel, J., Larsbo, M., 2016. Understanding preferential flow in the vadose zone: recent advances and future prospects. Vadose Zone J. 15 https://doi.org/10.2136/vzj2016.09.0075 vzj2016.09.0075.
Jégou, D., Brunotte, J., Rogasik, H., Capowiez, Y., Diestel, H., Schrader, S., Cluzeau, D., 2002. Impact of soil compaction on earthworm burrow systems using X-ray computed tomography: preliminary study. Eur. J. Soil Biol. 38, 329–336. https://doi.org/10.1016/S1164-5563(02)01148-2.
Kätterer, T., Börjesson, G., Kirchmann, H., 2014. Changes in organic carbon in topsoil and subsoil and microbial community composition caused by repeated additions of organic amendments and N fertilisation in a long-term field experiment in Sweden. Agric. Ecosyst. Environ. 189, 110–118. https://doi.org/10.1016/j.agee.2014.03.025.
Keller, T., Colombi, T., Ruiz, S., Manalili, M.P., Rek, J., Stadelmann, V., Wunderli, H., Breitenstein, D., Reiser, R., Oberholzer, H., Schymanski, S., Romero-Ruiz, A., Linde, N., Weisskopf, P., Walter, A., Or, D., 2017. Long-term soil structure observatory for monitoring post-compaction evolution of soil structure. Vadose Zone J. 16 https://doi.org/10.2136/vzj2016.11.0118 vzj2016.11.0118.
Klemmensen, N.D.R., Chand, R., Blanco, M.S., Vollertsen, J., 2024. Microplastic abundance in sludge-treated fields: Variance and estimated half-life. Sci. Total Environ. 171394 https://doi.org/10.1016/j.scitotenv.2024.171394.
Koutnik, V.S., Leonard, J., Brar, J., Cao, S., Glasman, J.B., Cowger, W., Ravi, S., Mohanty, S.K., 2022. Transport of microplastics in stormwater treatment systems under freeze-thaw cycles: Critical role of plastic density. Water Res. 222, 118950 https://doi.org/10.1016/j.watres.2022.118950.
Lares, M., Ncibi, M.C., Sillanpää, Markus, Sillanpää, Mika, 2018. Occurrence, identification and removal of microplastic particles and fibers in conventional activated sludge process and advanced MBR technology. Water Res. 133, 236–246. https://doi.org/10.1016/j.watres.2018.01.049.
Larsbo, M., Stenström, J., Etana, A., Börjesson, E., Jarvis, N.J., 2009. Herbicide sorption, degradation, and leaching in three Swedish soils under long-term conventional and reduced tillage. Soil Tillage Res. 105, 200–208. https://doi.org/10.1016/j.still.2009.08.003.
Larsson, M.H., Jarvis, N.J., 1999. Evaluation of a dual-porosity model to predict field-scale solute transport in a macroporous soil. J. Hydrol. 215, 153–171. https://doi.org/10.1016/S0022-1694(98)00267-4.
Leuther, F., Mikutta, R., Wolff, M., Kaiser, K., Schlüter, S., 2023. Structure turnover times of grassland soils under different moisture regimes. Geoderma 433, 116464. https://doi.org/10.1016/j.geoderma.2023.116464.
Li, X., Chen, L., Mei, Q., Dong, B., Dai, X., Ding, G., Zeng, E.Y., 2018. Microplastics in sewage sludge from the wastewater treatment plants in China. Water Res. 142, 75–85. https://doi.org/10.1016/j.watres.2018.05.034.
Liu, F., Olesen, K.B., Borregaard, A.R., Vollertsen, J., 2019. Microplastics in urban and highway stormwater retention ponds. Sci. Total Environ. 671, 992–1000. https://doi.org/10.1016/j.scitotenv.2019.03.416.
Ljung, E., Borg Olesen, K., Andersson, P.-G., Fältström, E., Vollertsen, J., Wittgren, H.B., Hagman, M., 2018. Mikroplaster i kretsloppet (No. 2018–13). Svenskt Vatten Utveckling.
Löder, M.G.J., Imhof, H.K., Ladehoff, M., Löschel, L.A., Lorenz, C., Mintenig, S., Piehl, S., Primpke, S., Schrank, I., Laforsch, C., Gerdts, G., 2017. Enzymatic purification of microplastics in environmental samples. Environ. Sci. Technol. 51, 14283–14292. https://doi.org/10.1021/acs.est.7b03055.
Lofty, J., Muhawenimana, V., Wilson, C.A.M.E., Ouro, P., 2022. Microplastics removal from a primary settler tank in a wastewater treatment plant and estimations of contamination onto European agricultural land via sewage sludge recycling. Environ. Pollut. 304, 119198 https://doi.org/10.1016/j.envpol.2022.119198.
Magnusson, K., Norén, F., 2014. Screening of Microplastic Particles in and Down-Stream a Wastewater Treatment Plant, IVL Report C.
Mahon, A.M., O'Connell, B., Healy, M.G., O'Connor, I., Officer, R., Nash, R., Morrison, L., 2017. Microplastics in sewage sludge: effects of treatment. Environ. Sci. Technol. 51, 810–818. https://doi.org/10.1021/acs.est.6b04048.
Martínez, I., Chervet, A., Weisskopf, P., Sturny, W.G., Etana, A., Stettler, M., Forkman, J., Keller, T., 2016. Two decades of no-till in the Oberacker long-term field experiment: Part I. Crop yield, soil organic carbon and nutrient distribution in the soil profile. Soil Tillage Res. 163, 141–151. https://doi.org/10.1016/j.still.2016.05.021.
McTavish, M.J., Murphy, S.D., 2021. Three-dimensional mapping of earthworm (Lumbricus terrestris) seed transport. Pedobiologia 87–88, 150752. https://doi.org/10.1016/j.pedobi.2021.150752.
Moreira, A., Moraes, L.A.C., de Melo, T.R., Heinrichs, R., Moretti, L.G., 2022. Chapter Five - management of copper for crop production. In: Sparks, D.L. (Ed.), Advances in Agronomy. Academic Press, pp. 257–298. https://doi.org/10.1016/bs.agron.2022.02.005.
Naturvårdsverket, 2009. Riktvärden För Förorenad Mark – Modellbeskrivning Och Vägledning. Naturvårdsverket, Stockholm.
O'Connor, D., Pan, S., Shen, Z., Song, Y., Jin, Y., Wu, W.-M., Hou, D., 2019. Microplastics undergo accelerated vertical migration in sand soil due to small size and wet-dry cycles. Environ. Pollut. 249, 527–534. https://doi.org/10.1016/j.envpol.2019.03.092.
Okoffo, E.D., Ribeiro, F., O'Brien, J.W., O'Brien, S., Tscharke, B.J., Gallen, M., Samanipour, S., Mueller, J.F., Thomas, K.V., 2020. Identification and quantification of selected plastics in biosolids by pressurized liquid extraction combined with double-shot pyrolysis gas chromatography–mass spectrometry. Sci. Total Environ. 715, 136924 https://doi.org/10.1016/j.scitotenv.2020.136924.
Prendergast-Miller, M.T., Katsiamides, A., Abbass, M., Sturzenbaum, S.R., Thorpe, K.L., Hodson, M.E., 2019. Polyester-derived microfibre impacts on the soil-dwelling earthworm Lumbricus terrestris. Environ. Pollut. 251, 453–459. https://doi.org/10.1016/j.envpol.2019.05.037.
Primpke, S., Cross, R.K., Mintenig, S.M., Simon, M., Vianello, A., Gerdts, G., Vollertsen, J., 2020a. Toward the systematic identification of microplastics in the environment: evaluation of a new independent software tool (siMPle) for spectroscopic analysis. Appl. Spectrosc. https://doi.org/10.1177/0003702820917760, 0003702820917760.
Primpke, S., Fischer, M., Lorenz, C., Gerdts, G., Scholz-Böttcher, B.M., 2020b. Comparison of pyrolysis gas chromatography/mass spectrometry and hyperspectral FTIR imaging spectroscopy for the analysis of microplastics. Anal. Bioanal. Chem. 412, 8283–8298. https://doi.org/10.1007/s00216-020-02979-w.
Primpke, S., Lorenz, C., Rascher-Friesenhausen, R., Gerdts, G., 2017. An automated approach for microplastics analysis using focal plane array (FPA) FTIR microscopy and image analysis. Anal. Methods 9, 1499–1511. https://doi.org/10.1039/C6AY02476A.
Qi, S., Song, J., Shentu, J., Chen, Q., Lin, K., 2022. Attachment and detachment of large microplastics in saturated porous media and its influencing factors. Chemosphere 305, 135322. https://doi.org/10.1016/j.chemosphere.2022.135322.
Qiu, Y., Zhou, S., Zhang, C., Chen, L., Qin, W., Zhang, Q., 2023. Vertical distribution and weathering characteristic of microplastics in soil profile of different land use types. Sci. Total Environ. 905, 166902 https://doi.org/10.1016/j.scitotenv.2023.166902.
Ranjan, V.P., Joseph, A., Sharma, H.B., Goel, S., 2023. Preliminary investigation on effects of size, polymer type, and surface behaviour on the vertical mobility of microplastics in a porous media. Sci. Total Environ. https://doi.org/10.1016/j.scitotenv.2022.161148.
Ren, Z., Gui, X., Wei, Y., Chen, X., Xu, X., Zhao, L., Qiu, H., Cao, X., 2021. Chemical and photo-initiated aging enhances transport risk of microplastics in saturated soils: Key factors, mechanisms, and modeling. Water Res. 202, 117407 https://doi.org/10.1016/j.watres.2021.117407.
Rillig, M.C., Ziersch, L., Hempel, S., 2017. Microplastic transport in soil by earthworms. Sci. Rep. 7, 1362. https://doi.org/10.1038/s41598-017-01594-7.
Sauvé, S., Hendershot, W., Allen, H.E., 2000. Solid-solution partitioning of metals in contaminated soils: dependence on pH, total metal burden, and organic matter. Environ. Sci. Technol. 34, 1125–1131. https://doi.org/10.1021/es9907764.

Schell, T., Hurley, R., Buenaventura, N.T., Mauri, P.V., Nizzetto, L., Rico, A., Vighi, M., 2022. Fate of microplastics in agricultural soils amended with sewage sludge: is surface water runoff a relevant environmental pathway? Environ. Pollut. 293, 118520 https://doi.org/10.1016/j.envpol.2021.118520.
Schlüter, S., Albrecht, L., Schwärzel, K., Kreiselmeier, J., 2020. Long-term effects of conventional tillage and no-tillage on saturated and near-saturated hydraulic conductivity – can their prediction be improved by pore metrics obtained with X-ray CT? Geoderma 361, 114082. https://doi.org/10.1016/j.geoderma.2019.114082.
Simon, M., Alst, N. van, Vollertsen, J., 2018. Quantification of microplastic mass and removal rates at wastewater treatment plants applying Focal Plane Array (FPA)-based Fourier Transform Infrared (FT-IR) imaging. Water Res. 142, 1–9. https://doi.org/10.1016/j.watres.2018.05.019.
Steinmetz, Z., Kintzi, A., Muñoz, K., Schaumann, G.E., 2020. A simple method for the selective quantification of polyethylene, polypropylene, and polystyrene plastic debris in soil by pyrolysis-gas chromatography/mass spectrometry. J. Anal. Appl. Pyrolysis 104803. https://doi.org/10.1016/j.jaap.2020.104803.
Steinmetz, Z., Löffler, P., Eichhöfer, S., David, J., Muñoz, K., Schaumann, G.E., 2022. Are agricultural plastic covers a source of plastic debris in soil? A first screening study. SOIL 8, 31–47. https://doi.org/10.5194/soil-8-31-2022.
Tagg, A.S., Brandes, E., Fischer, F., Fischer, D., Brandt, J., Labrenz, M., 2022. Agricultural application of microplastic-rich sewage sludge leads to further uncontrolled contamination. Sci. Total Environ. 806, 150611 https://doi.org/10.1016/j.scitotenv.2021.150611.
Taylor, A.R., Lenoir, L., Vegerfors, B., Persson, T., 2018. Ant and earthworm bioturbation in cold-temperate ecosystems. Ecosystems 22, 981–994. https://doi.org/10.1007/s10021-018-0317-2.
Thomas, D., Schütze, B., Heinze, W.M., Steinmetz, Z., 2020. Sample preparation techniques for the analysis of microplastics in soil - a review. Sustainability 12, 9074. https://doi.org/10.3390/su12219074.
Thornton Hampton, L.M., Brander, S.M., Coffin, S., Cole, M., Hermabessiere, L., Koelmans, A.A., Rochman, C.M., 2022. Characterizing microplastic hazards: which concentration metrics and particle characteristics are most informative for understanding toxicity in aquatic organisms? Microplastics Nanoplastics 2, 20. https://doi.org/10.1186/s43591-022-00040-4.
Toapanta, T., Okoffo, E.D., Ede, S., O'Brien, S., Burrows, S.D., Ribeiro, F., Gallen, M., Colwell, J., Whittaker, A.K., Kaserzon, S., Thomas, K.V., 2021. Influence of surface oxidation on the quantification of polypropylene microplastics by pyrolysis gas chromatography mass spectrometry. Sci. Total Environ. 796, 148835 https://doi.org/10.1016/j.scitotenv.2021.148835.
Torppa, K.A., Taylor, A.R., 2022. Alternative combinations of tillage practices and crop rotations can foster earthworm density and bioturbation. Appl. Soil Ecol. 175, 104460 https://doi.org/10.1016/j.apsoil.2022.104460.
van den Berg, P., Huerta-Lwanga, E., Corradini, F., Geissen, V., 2020. Sewage sludge application as a vehicle for microplastics in eastern Spanish agricultural soils. Environ. Pollut. 261, 114198 https://doi.org/10.1016/j.envpol.2020.114198.
van Straalen, N.M., Schobben, J.H.M., de Goede, R.G.M., 1989. Population consequences of cadmium toxicity in soil microarthropods. Ecotoxicol. Environ. Saf. 17, 190–204. https://doi.org/10.1016/0147-6513(89)90038-9.
Viitala, M., Steinmetz, Z., Sillanpää, Mika, Mänttäri, M., Sillanpää, Markus, 2022. Historical and current occurrence of microplastics in water and sediment of a Finnish lake affected by WWTP effluents. Environ. Pollut. 314, 120298 https://doi.org/10.1016/j.envpol.2022.120298.
Viketoft, M., Riggi, L.G.A., Bommarco, R., Hallin, S., Taylor, A.R., 2021. Type of organic fertilizer rather than organic amendment per se increases abundance of soil biota. PeerJ 9, e11204. https://doi.org/10.7717/peerj.11204.
Wahl, A., Davranche, M., Rabiller-Baudry, M., Pédrot, M., Khatib, I., Labonne, F., Canté, M., Cuisinier, C., Gigault, J., 2024. Condition of composted microplastics after they have been buried for 30 years: vertical distribution in the soil and degree of degradation. J. Hazard Mater. 462, 132686 https://doi.org/10.1016/j.jhazmat.2023.132686.
Wasserstein, R.L., Schirm, A.L., Lazar, N.A., 2019. Moving to a world beyond "$p < 0.05$.". Am. Statistician 73, 1–19. https://doi.org/10.1080/00031305.2019.1583913.
Weber, C.J., Opp, C., 2020. Spatial patterns of mesoplastics and coarse microplastics in floodplain soils as resulting from land use and fluvial processes. Environ. Pollut. 267, 115390 https://doi.org/10.1016/j.envpol.2020.115390.
Weber, C.J., Opp, C., Prume, J.A., Koch, M., Andersen, T.J., Chifflard, P., 2021. Deposition and in-situ translocation of microplastics in floodplain soils. Sci. Total Environ. 152039 https://doi.org/10.1016/j.scitotenv.2021.152039.
Weber, C.J., Santowski, A., Chifflard, P., 2022. Investigating the dispersal of macro- and microplastics on agricultural fields 30 years after sewage sludge application. Sci. Rep. 12, 6401. https://doi.org/10.1038/s41598-022-10294-w.
Wenig, P., Odermatt, J., 2010. OpenChrom: a cross-platform open source software for the mass spectrometric analysis of chromatographic data. BMC Bioinf. 11, 405. https://doi.org/10.1186/1471-2105-11-405.
Yu, M., van der Ploeg, M., Lwanga, E.H., Yang, X., Zhang, S., Ma, X., Ritsema, C.J., Geissen, V., 2019. Leaching of microplastics by preferential flow in earthworm (Lumbricus terrestris) burrows. Environ. Chem. 16, 31–40. https://doi.org/10.1071/EN18161.
Zhang, L., Xie, Y., Liu, J., Zhong, S., Qian, Y., Gao, P., 2020. An overlooked entry pathway of microplastics into agricultural soils from application of sludge-based fertilizers. Environ. Sci. Technol. 54, 4248–4255. https://doi.org/10.1021/acs.est.9b07905.
Zhang, X., Chen, Y., Li, X., Zhang, Y., Gao, W., Jiang, J., Mo, A., He, D., 2022. Size/shape-dependent migration of microplastics in agricultural soil under simulative and natural rainfall. Sci. Total Environ. 815, 152507 https://doi.org/10.1016/j.scitotenv.2021.152507.
Zhang, Y.-Q., Lykaki, M., Markiewicz, M., Alrajoula, M.T., Kraas, C., Stolte, S., 2022. Environmental contamination by microplastics originating from textiles: Emission, transport, fate and toxicity. J. Hazard Mater. 430, 128453 https://doi.org/10.1016/j.jhazmat.2022.128453.
Zhao, Z., Zhao, K., Zhang, T., Xu, Y., Chen, R., Xue, S., Liu, M., Tang, D., Yang, X., Giessen, V., 2022. Irrigation-facilitated low-density polyethylene microplastic vertical transport along soil profile: an empirical model developed by column experiment. Ecotoxicol. Environ. Saf. https://doi.org/10.1016/j.ecoenv.2022.114232.
Zheljazkov, V.D., Warman, P.R., 2004. Phytoavailability and fractionation of copper, manganese, and zinc in soil following application of two composts to four crops. Environ. Pollut. 131, 187–195. https://doi.org/10.1016/j.envpol.2004.02.007.
Zhou, J., Wang, Y., Tong, Y., Sun, H., Zhao, Y., Zhang, P., 2023. Regional spatial variability of soil organic carbon in 0–5 m depth and its dominant factors. Catena 231, 107326. https://doi.org/10.1016/j.catena.2023.107326.